TOXICOLOGICAL SCIENCES **98(1)**, 216–230 (2007)
doi:10.1093/toxsci/kfm087
Advance Access publication April 13, 2007

Cyclophosphamide-Induced Apoptosis in COV434 Human Granulosa Cells Involves Oxidative Stress and Glutathione Depletion

Miyun Tsai-Turton,* Brian T. Luong,† Youming Tan,†,‡ and Ulrike Luderer*,†,§,[1]

*Department of Community and Environmental Medicine; †Department of Medicine, University of California, Irvine, California 92617; ‡Department of Environmental Health, School of Public Health, Shanghai Jiaotong University, Shanghai, China; and §Department of Developmental and Cell Biology, University of California, Irvine, California 92617

Received November 2, 2006; accepted April 10, 2007

The anticancer drug cyclophosphamide induces granulosa cell apoptosis and is detoxified by glutathione (GSH) conjugation. We previously showed that both cyclophosphamide treatment and GSH depletion induced granulosa cell apoptosis in rats, but the role of GSH in apoptosis in human ovarian cells has not been studied. Using the COV434 human granulosa cell line, we tested the hypotheses that (1) GSH depletion or treatment with 4-hydroperoxycyclophosphamide (4HC), a preactivated form of cyclophosphamide, induces apoptosis, (2) GSH depletion potentiates 4HC-induced apoptosis, and (3) 4HC-induced apoptosis is mediated by GSH depletion and oxidative stress. Cells were treated with buthionine sulfoximine (BSO), a specific inhibitor of GSH synthesis, with or without follicle stimulating hormone (FSH) or serum. A significant increase in the number of apoptotic cells, assessed by terminal deoxynucleotidyl transferase–mediated deoxy-uridine triphosphate nick-end labeling (TUNEL) and Hoechst 33342 staining, occurred with BSO treatment. Treatment with 4HC dose-dependently induced apoptosis by TUNEL, Hoechst staining, and caspase 3 activation. Treatment with 4HC caused an increase in reactive oxygen species generation, measured by dichlorofluorescein fluorescence, oxidative DNA damage, measured by 8-hydroxyguanosine immunostaining, and an oxidation of the redox potential for the oxidized glutathione/reduced glutathione couple. Total intracellular GSH declined after 4HC treatment, preceding the onset of cell death. Treatment with antioxidants inhibited 4HC-induced apoptosis. Combined treatment with BSO and 4HC caused greater induction of apoptosis than either treatment alone. These findings are consistent with roles for oxidative stress and GSH depletion in mediating the induction of apoptosis in COV434 cells by cyclophosphamide.

Key Words: **granulosa cell; glutathione; cyclophosphamide; apoptosis; 4-hydroperoxycyclophosphamide; oxidative stress; ovary; antioxidant.**

The anticancer drug cyclophosphamide causes amenorrhea and premature ovarian failure in women (Howell and Shalet, 1998; Kumar *et al.*, 1972). Studies in rodents suggest that cyclophosphamide disrupts ovarian function by destroying ovarian follicles. Cyclophosphamide treatment destroys ovarian follicles in mice and rats (Davis and Heindel, 1998; Plowchalk and Mattison, 1991, 1992; Shiromizu *et al.*, 1984). Although mice are more sensitive to the effects of cyclophosphamide on the immature primordial and primary follicles, cyclophosphamide targets granulosa cells of more mature, antral follicles in both mice and rats (Davis and Heindel, 1998; Plowchalk and Mattison, 1991, 1992; Shiromizu *et al.*, 1984). We have shown that the destruction of granulosa cells by cyclophosphamide in rats treated *in vivo* occurs by the induction of apoptosis (Lopez and Luderer, 2004). Both the death receptor and the mitochondrial apoptotic pathways have been implicated in the induction of apoptosis by cyclophosphamide in developing embryos (Little and Mirkes, 2002; Mirkes and Little, 2000) and hair follicles (Lindner *et al.*, 1997). However, the mechanism by which cyclophosphamide induces granulosa cell apoptosis has not been investigated. The mitochondrial apoptotic pathway is initiated by damaging stimuli such as oxidative stress or DNA damage (Coppola and Ghibelli, 2000). Cyclophosphamide's therapeutic mechanism of action as an alkylating agent induces DNA damage (Gamcsik *et al.*, 1999). Cyclophosphamide treatment has also been shown to cause oxidative stress (Berrigan *et al.*, 1987; Murata *et al.*, 2004; Venkatesan and Chandrakasan, 1995). In the present studies we focused on oxidative stress as a mediator of cyclophosphamide-induced granulosa cell apoptosis.

The tripeptide glutathione (GSH) is the most abundant intracellular nonprotein thiol. GSH serves numerous physiological functions including detoxification of reactive oxygen species (ROS), acting as a cofactor for enzymes, serving as a storage form for cysteine, and regulating protein and DNA synthesis by altering redox status (Dalton *et al.*, 2004). Moreover, GSH conjugation is a critical Phase II biotransformation mechanism for exogenous toxicants. GSH depletion induces apoptosis in some cell types in culture (Anderson *et al.*,

[1] To whom correspondence should be addressed at Center for Occupational and Environmental Health, 5201 California Avenue, Suite 100, Irvine, CA 92617. Fax: (949) 824-2345. E-mail: uluderer@uci.edu.

1999; Celli *et al.*, 1998; Higuchi and Matsukawa, 1999; Merad-Boudia *et al.*, 1998). In other cell types, GSH depletion sensitizes cells to proapoptotic stimuli (Schnelldorfer *et al.*, 2000; Wright *et al.*, 1998). *In vivo* suppression of GSH synthesis with buthionine sulfoximine (BSO) significantly increased antral follicle atresia, an apoptotic process of degeneration, in adult rat ovaries (Lopez and Luderer, 2004). In cultured preovulatory rat follicles, GSH depletion with BSO partially reversed the antiapoptotic effect of follicle stimulating hormone (FSH) on granulosa cells (Tsai-Turton and Luderer, 2006).

Cyclophosphamide requires metabolic activation via oxidation by cytochrome P450 enzymes (CYP2A6, -2B6, -2C8, -2C9, and -3A4) to 4-hydroxycyclophosphamide (Chang *et al.*, 1993; Dirven *et al.*, 1994; Gamcsik *et al.*, 1999). 4-Hydroxycyclophosphamide undergoes ring opening to aldophosphamide, which spontaneously decomposes to the reactive metabolite phosphoramide mustard (Dirven *et al.*, 1994; Gamcsik *et al.*, 1999). Phosphoramide mustard is thought to be the active metabolite both in terms of anticancer activity and in terms of ovarian toxicity (Gamcsik *et al.*, 1999; Plowchalk and Mattison, 1991). Cyclophosphamide itself, phosphoramide mustard, and other metabolites are detoxified by conjugation with GSH (Dirven *et al.*, 1994; Gamcsik *et al.*, 1999).

COV434 cells are derived from a human granulosa cell tumor; however, they possess many of the characteristics of normal granulosa cells, including cyclic-adenosine monophosphate production in response to FSH stimulation, estradiol synthesis in response to FSH and androstenedione, and formation of intercellular connections with cumulus cells surrounding a human oocyte (Zhang *et al.*, 2000). Herein we describe experiments conducted using these cells to test the hypotheses that (1) GSH depletion and cyclophosphamide treatment induce apoptosis in human granulosa cells, (2) GSH depletion sensitizes human granulosa cells to the induction of apoptosis by cyclophosphamide, and (3) cyclophosphamide treatment causes GSH depletion and oxidative stress in granulosa cells, which mediate the induction of apoptosis.

MATERIALS AND METHODS

Materials. All chemicals were purchased from Sigma-Aldrich (St Louis, MO) or Fisher Scientific (Pittsburgh, PA), unless otherwise noted. Tissue culture reagents and Mycotect Kit were from Invitrogen (Carlsbad, CA). Recombinant human FSH (FSH; IOD/BIO Lot#AFP-8468A, 6650 IU/mg) was obtained from Dr A. F. Parlow, National Hormone and Peptide Program, NIDDK. WST-1 reagent, diaminobenzidine substrate and buffer, and *In situ* Cell Death Detection Kit POD were from Roche Applied Science (Indianapolis, IN). The DNeasy DNA extraction kit was from Qiagen (Valencia, CA). The 4-hydroperoxycyclophosphamide (4HC) was a gift of Dr Susan Ludeman, Duke University Medical Center, Durham, NC. Additional 4HC was purchased from IIT GmbH, part NIOMECH (Bielefeld, Germany).

COV434 human granulosa cell culture. COV434 cells (gift of Dr Peter Schrier, University Hospital of Leiden, Netherlands) are derived from a human granulosa cell tumor (van den Berg-Bakker *et al.*, 1993), but possess many characteristics of normal granulosa cells (Zhang *et al.*, 2000). A preliminary dose–response experiment showed that culture for 24 h with concentrations of BSO from 100 to 1000μM suppressed intracellular GSH to less than 15% of control levels, whereas 5 and 20μM concentrations suppressed GSH to 15% and 26% of control levels, respectively (data not shown). Depletion of GSH to less than 10% of control levels caused apoptosis in various cell types (Celli *et al.*, 1998; Higuchi and Matsukawa, 1999; Merad-Boudia *et al.*, 1998), whereas depletion of GSH to about 27% of control levels did not cause apoptosis in another study (Jungas *et al.*, 2002). Therefore, to increase the likelihood of inducing apoptosis, 100μM BSO was used for the subsequent experiments.

COV434 cells were maintained in Dulbecco's modified Eagle's medium (DMEM) F12 with GlutaMAX and 9% fetal bovine serum (complete medium). Cells were routinely assessed for mycoplasma contamination using the Mycotect Kit and were found to be free of contamination. During maintenance, cells were passaged every 4–5 days. Cells from passages 34–77 were used for the experiments reported herein. For experiments, cells were harvested by trypsinization, counted using a hemacytometer, and were plated in complete medium. For DNA or protein extraction COV434 cells were plated 7×10^6 cells per 75-cm^2 flask for 24 h treatment or 5×10^6 cells/flask for 48–96 h treatment. For GSH assay, cells were plated 2.5×10^6 cells per 25-cm^2 flask. Cells were plated 5×10^4 cells per chamber of eight-chamber Lab-Tek II CC2 tissue culture slides (Nunc, Roskilde, Denmark) for TUNEL, Hoechst 33342 staining, or immunofluorescence. Cells were plated 2×10^4 cells per well of a 96-well plate for WST-1 cell viability assay and 3×10^4 cells per well for ROS assay.

For the experiments testing the effects of GSH depletion on apoptosis in COV434 cells, the complete medium was removed after 24 h, cells were washed twice with phosphate buffered saline (PBS), and the treatment media were added. All or a subset of the following treatment groups were included: (1) serum-free control medium alone (DMEM F12), (2) DMEM F12 plus 100μM BSO, (3) 50 ng/ml FSH, (4) 200 ng/ml FSH, (5) 50 ng/ml FSH plus 100μM BSO, (6) 200 ng/ml FSH plus 100μM BSO, (7) DMEM F12 with 9% FBS, and (8) DMEM F12 with FBS plus 100μM BSO. For experiments testing the effects of 4HC on apoptosis, COV434 cells were cultured for 24 h in complete medium before the addition of 4HC dissolved in medium. Final concentrations of 4HC in the culture dishes were 0, 1, 10, or 50μM. Additional experiments included groups that were cotreated with 4HC and 100μM BSO or with 4HC and one of three antioxidants. The concentrations of antioxidants were 5mM glutathione ethyl ester (GEE), a cell-permeable form of GSH, 0.5mM dithiothreitol (DTT), a thiol antioxidant, or 1mM ascorbic acid (AA) (Higuchi and Matsukawa, 1999; Merad-Boudia *et al.*, 1998; Puri and Meister, 1983; Tsai-Turton and Luderer, 2006). Plasma concentrations of 1–10μM of the 4-hydroxycyclophosphamide metabolite of cyclophosphamide, to which 4HC spontaneously decomposes, have been reported in patients receiving infusions of cyclophosphamide prior to bone marrow transplantation (Ren *et al.*, 1998).

GSH assay. After treatment, cells were harvested by trypsinization, counted with a hemacytometer and trypan blue, and centrifuged at 300 × g for 5 min. Cell pellets were lysed using a Kontes pellet pestle homogenizer in buffer containing 20mM Tris base, 1mM ethylenediaminetetraacetic acid (EDTA), 250mM sucrose, 2mM L-serine, and 20mM borate for 30 s on ice. After removing an aliquot of suspension for protein assay with a bicinchoninic acid (BCA) assay kit (Pierce, Rockford, IL), 1/4 volume 5% sulfosalicylic acid was added. After 15 min incubation on ice, cell suspensions were centrifuged at 15,800 × g for 10 min at 4°C. Total GSH and GSSG concentrations in the supernatants were measured using a modification (Luderer *et al.*, 2001; Tsai-Turton and Luderer, 2005, 2006) of an enzymatic recycling assay developed by Griffith (1980). The concentration of reduced glutathione (rGSH) was calculated as the total GSH concentration in the sample minus two times the GSSG concentration. The interassay coefficient of variation (CV), calculated from a pool that was run in every assay, was 16.8% for total GSH, and 4.5% for GSSG. The intra-assay CVs ranged from 4.0% to 13.4% for total GSH and from 3.0% to 4.9% for GSSG.

The GSH reduction potential was calculated using the Nernst Equation:

$$E_h = (E_0 - ((RT/nF)\ln([\mathrm{GSH}]^2/[\mathrm{GSSG}]))$$

$$E_0 = E_0 - 61.5\,\text{mV}/1.0\,\text{unit increase in pH}\,(\text{pH}_{\text{actual}} - \text{pH}_{\text{standard}}) = 264.6\,\text{for pH}\,7.4$$

where $E_0 = -240$ mV; R is the universal gas constant (831 J/K/mol); T is the temperature in Kelvin (310 K is 37°C); n is the number of electrons transferred (two in this case); F is the Faraday constant (9.65 Coulombs $\times$ 10^4/mol); and the concentrations of GSH and GSSG in molar units were estimated from the concentrations in nanomoles/10^6 cells by assuming a volume of 1.14 μl per 10^6 cells (Dhar *et al.*, 1996; Kirlin *et al.*, 1999; Schafer and Buettner, 2001; Shen *et al.*, 2005).

Terminal deoxynucleotidyl transferase-mediated deoxy-uridine triphosphate nick-end-labeling (TUNEL). At the end of the treatment period, cells were washed twice with ice-cold PBS, fixed for 30 min with 4% paraformaldehyde on ice, washed again with cold PBS, and subjected to TUNEL. TUNEL was performed using the *In Situ* Cell Death Detection Kit POD essentially as described (Luderer *et al.*, 2003), with the following modifications. The terminal transferase was diluted one part terminal transferase to nine parts fluorescein-conjugated deoxy-uridine triphosphate label solution and 10 parts TUNEL dilution buffer. The peroxidase converter solution was diluted 2:1 peroxidase solution to TUNEL dilution buffer.

TUNEL-positive cells and TUNEL-negative cells (counterstained with hematoxylin) were counted in three ×400 fields per chamber. The average percentage of TUNEL-positive cells was calculated for each chamber and was used for data presentation and for statistical analyses.

Hoechst 33342 staining for apoptosis. The bisbenzamide dye, Hoechst 33342, was used for detection of apoptotic cells. At the end of the treatment period, cells were washed and fixed as for TUNEL. Slides were then immediately stained with 50 μg/ml Hoechst 33342 dye diluted in PBS for 10 min in the dark, rinsed with distilled water, and allowed to dry in the dark. Slides were coverslipped with Mowiol mounting agent and viewed using an Olympus BX60 microscope equipped for fluorescence microscopy at an excitation wavelength of 355 nm and an emission wavelength of 465 nm. Cells with intensely fluorescent and/or fragmented nuclei were considered apoptotic (Zhivotovsky and Orrenius, 2001). Apoptotic cells were counted in three ×200 fields per chamber, and the average was used for data presentation and statistical analyses.

Protein extraction, gel electrophoresis, and immunoblotting. Cells were harvested by trypsinization and collected into complete medium to deactivate trypsin. After centrifugation of trypsinized cells and growth medium containing detached cells at 300 × g for 5 min, cell pellets were washed with PBS, then lysed on ice in RIPA buffer (PBS, 1% Nonidet-P-40, 0.1% deoxycholate, 0.1% sodium dodecyl sulfate) with protease inhibitors. Lysates were incubated on ice for 30 min and centrifuged at 15,800 × g for 10 min at 4°C. Protein concentrations in supernatants were measured using a BCA assay kit (Pierce, Rockford, IL), and 40 μg of protein per lane was separated by electrophoresis in 12% Tris–HCl polyacrylamide gels (BioRad, Hercules, CA). The proteins were transferred to polyvinylidine difluoride membranes, and immunoblotting was performed essentially as described (Luderer *et al.*, 2001) using an activated caspase 3 antibody (Asp175, Cell Signaling, Beverly, MA) at a dilution of 1:100, followed by reprobing with β-actin antiserum (Sigma-Aldrich) as a loading control.

DNA extraction and gel electrophoresis. At the end of the treatment period, cells were collected by scraping with a cell scraper, followed by centrifugation at 300 × g to pellet the cells. Pellets were then washed with PBS, centrifuged again, and were stored at −70°C until DNA extraction using the DNeasy Kit according to the manufacturer's instructions. Ten micrograms of DNA from each sample was separated by electrophoresis in 2% agarose gels made with modified Tris–acetate–EDTA buffer with 0.5 μg/ml ethidium bromide. Visualization was accomplished by ultraviolet transillumination.

Cell viability WST-1 assay. Cell viability was based on the cleavage of the tetrazolium salt WST-1 to formazan by mitochondrial dehydrogenases of viable COV434 granulosa cells. At the end of the treatment periods, 10 μl of WST-1 reagent was added to each well, and the plate was incubated for 2 h at 37°C in a humidified atmosphere of 95% air, 5% CO_2. The absorbance at 440 nm was then read using a VersaMax Tunable Microplate Reader (Molecular Devices, Sunnyvale, CA). The absorbance of the average of three blank wells containing medium and WST-1 reagent with no cells was subtracted from each absorbance reading, and the resulting values were used for data analysis and presentation.

Immunofluorescence. Oxidative DNA damage was assessed using 8-hydroxy-2′-deoxyguanosine (8-OHdG) immunofluorescence. Treated cells were washed with PBS, fixed and permeabilized with 70% methanol for 5 min on ice, followed by 100% methanol for 20 min at −70°C, and washed again with PBS. Slides were blocked for 30 min with 10% normal goat serum in PBS, washed in PBS, incubated for 1 h with monoclonal anti-8-OHdG antibody (1:500; Clone 4E9, Trevigen, Gaithersburg, MD), washed, incubated with fluorescein-conjugated goat anti-mouse IgG H + L (1:100; #115-095-146; Jackson ImmunoResearch, West Grove, PA) for 1 h, washed, coverslipped with Vectashield mounting medium, and viewed with an Olympus BX60 microscope equipped for epifluorescence. The number of positively stained cells was counted in two ×200 fields per well, and the average was used for data presentation and statistical analyses.

ROS detection by dichlorofluorescein diacetate assay. Dichlorofluorescein diacetate (DCF-DA) is taken up by cells, is cleaved to DCF by intracellular esterases, and is oxidized in the presence of ROS to DCF (Royall and Ischiropoulos, 1993). Modifications of a previously described DCF-DA microplate assay were used to measure ROS after 4HC treatment (Wang and Joseph, 1999). Cells were cultured 3 × 10^4 cells per well of a 96-well plate in 100 μl of complete medium for 24 h. For measurement of the acute effect of 4HC treatment on ROS generation, the wells were washed with PBS, loaded for 30 min at 37°C with 100μM DCF-DA in medium, washed again, and treated with 0, 1, 10, or 50μM 4HC or 500μM hydrogen peroxide as a positive control in Hanks Balanced Salt Solution while fluorescence intensity was measured every 5 min for 2 h using a Biotek FL600 spectrofluorometer microplate reader (Biotek Instruments, Winooski, VT) with excitation wavelength set at 485 nm, emission wavelength set at 530 nm, and temperature set at 37°C. For measurement of ROS at a later time point, 10 μl of medium containing 4HC to give a final concentration of 0, 1, 10, or 50μM was added to each well after the 24-h preincubation period, and the plate was returned to the incubator for 6 h. After washing with PBS, 100 μl of medium containing 100μM DCF-DA was added. After incubation at 37°C for 30 min, the DCF-DA containing medium was removed, cells were washed with PBS, and maintained in PBS while fluorescence intensity was read as above.

Estradiol radioimmunoassay. For the experiments assessing the effect of FSH treatment on estradiol synthesis, 7 × 10^6 cells were plated per 75-cm^2 flask for 24 h treatment or 5 × 10^6 cells/flask for 72 h treatment. After 24 h in complete medium, the cells were washed and treated with one of the following in DMEM F12 medium: (1) medium alone, (2) 200 ng/ml FSH, or (3) FSH plus 10μM androstenedione (Zhang *et al.*, 2000). At the end of the treatment period, an aliquot of medium was removed and stored at −70°C until estradiol assay. Estradiol was measured using reagents from the Estradiol Double Antibody Radioimmunoassay Kit from Diagnostic Products Corporation (Los Angeles, CA), except that a standard curve was generated in DMEM F12 medium (0, 9, 18, 72, 145, 289, and 578 pg/ml). All of the samples were measured in a single assay. The intraassay CV was 8.5%.

Statistical analyses. Data from replicate experiments were pooled for statistical analyses. Differences among treatment groups were evaluated by analysis of variance (ANOVA) for each time point. The proportions of TUNEL-positive cells were subjected to arcsine square root transformations (Pasternack and Shore, 1982) and then analyzed by ANOVA. If the overall p-value indicated statistical significance ($p < 0.05$), *post hoc* least significant difference (LSD) tests were applied to assess differences among groups based on *a priori* hypotheses. Levene's test was used to assess homogeneity of variances. If variances were not homogeneous, the natural logarithm transformation was applied. If variances were still not homogenous, the Kruskal–Wallis test was used to assess the overall effect of treatment. If the latter was statistically significant at $p < 0.05$, the Mann–Whitney test was then used for intergroup comparisons. SPSS Version 13.0 for Macintosh was used for all statistical analyses.

RESULTS

Effect of FSH and BSO Treatment on Intracellular GSH Concentrations in Cultured COV434 Human Granulosa Cells

COV434 cells are responsive to FSH stimulation in our hands, as indicated by the increase in estradiol synthesis when treated with 10μM androstenedione and 200 ng/ml FSH (Fig. 1). FSH treatment appeared to modestly increase intracellular GSH levels at 24 h, but not at later time points (Fig. 2A). This contrasts with the pronounced stimulatory effect of FSH we have observed on GSH synthesis in cultured rat preovulatory follicles (Tsai-Turton and Luderer, 2006). Combined treatment with FSH and androstenedione also did not increase GSH concentrations relative to cells cultured in medium alone (data not shown). Treatment with BSO suppressed intracellular GSH levels to 15% of control levels after 24 h and to less than 5% of control levels at later time points ($p < 0.001$, effect of treatment; $p = 0.117$, effect of time by two-way ANOVA; Fig. 2A). Figure 2B shows that intracellular GSH concentrations were significantly decreased compared to 0 h control levels by 2 h after the onset of treatment with 100μM BSO and were suppressed to 50% of 0 h levels after 8 h of BSO treatment.

Effect of FSH and BSO Treatment on Apoptosis in Cultured COV434 Human Granulosa Cells

GSH depletion with BSO has been shown to induce apoptosis in some (Anderson *et al.*, 1999; Celli *et al.*, 1998; Higuchi and Matsukawa, 1999; Merad-Boudia *et al.*, 1998), but not all (Schnelldorfer *et al.*, 2000; Wright *et al.*, 1998), cell types that have been investigated. The effect of GSH depletion on apoptosis in COV434 cells was investigated using TUNEL, Hoechst 33342 staining, and DNA gel electrophoresis.

Cotreatment with FSH and BSO or treatment with BSO alone led to a time-dependent and statistically significant increase in the percentage of TUNEL-positive cells, with nearly 100% of BSO-treated cells TUNEL positive after 96 h of treatment ($p < 0.004$, effect of BSO by two-way ANOVA; $p < 0.008$, effect of treatment by Kruskal–Wallis test at 24, 48, 72, and 96 h; Figs. 3A and 3B). The effect of FSH treatment was not statistically significant at any time point.

Staining of COV434 cells with Hoechst 33342 dye verified that cell death was apoptotic and not necrotic, as judged by

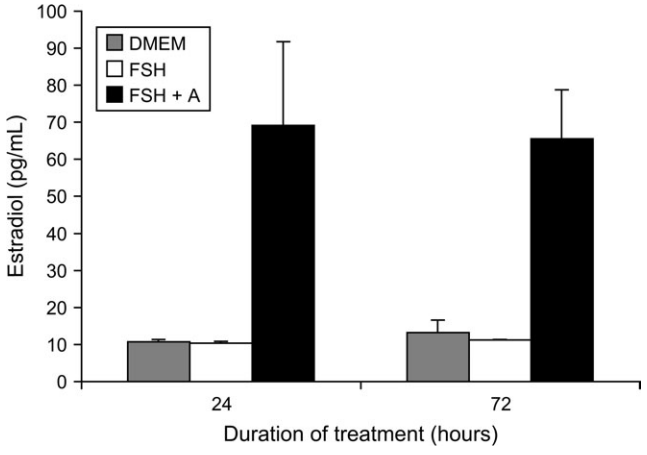

FIG. 1. Treatment of COV434 cells with FSH and androstenedione stimulates estradiol synthesis. COV434 cells were cultured in (1) serum-free medium alone (DMEM), (2) with 200 ng/ml FSH, (3) or with FSH plus 10μM androstenedione (FSH + A). At the end of the indicated treatment periods, media were collected, and estradiol concentrations were measured by radioimmunoassay. Cotreatment with FSH and androstenedione significantly increased estradiol concentrations in the media ($p = 0.008$, $p = 0.024$, effect of treatment by Kruskal–Wallis test at 24 and 72 h, respectively).

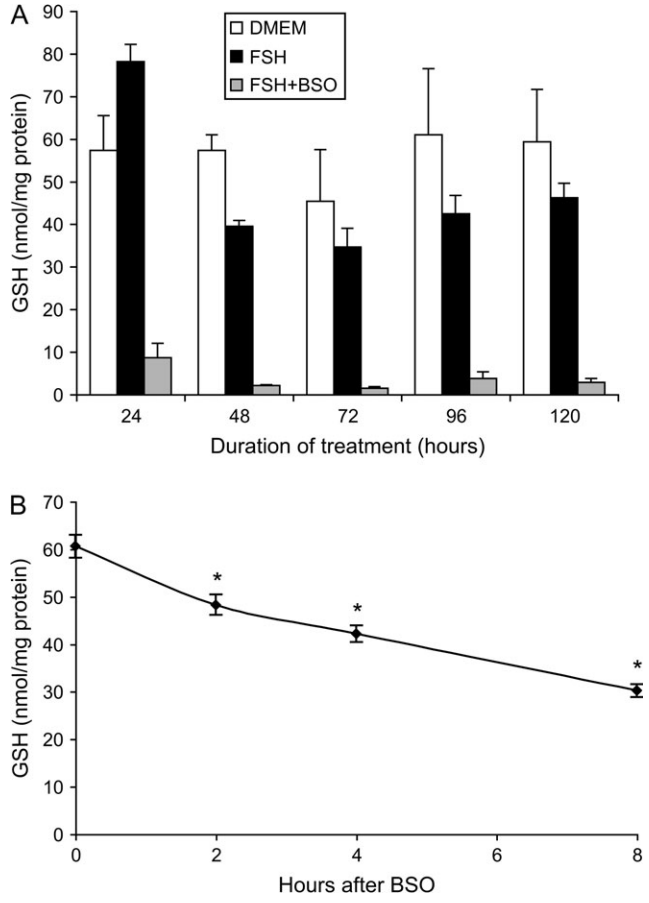

FIG. 2. Time course of suppression of total intracellular GSH concentrations after BSO treatment. (A) COV434 cells were cultured in (1) DMEM F12 medium (DMEM), (2) with 200 ng/ml FSH (FSH), or (3) with 200 ng/ml FSH plus 100μM BSO (FSH + BSO). At the end of the indicated treatment periods, cells were collected for assay of total intracellular GSH. The effect of treatment was statistically significant overall ($p < 0.001$, effect of treatment; $p = 0.117$, effect of time by two-way ANOVA). Treatment with BSO significantly suppressed GSH at all time points tested ($p < 0.001$, FSH + BSO vs. FSH and DMEM). (B) COV434 cells were cultured with 100μM BSO in DMEM F12 medium for 0, 2, 4, or 8 h ($N = 4$–6 per group). The effect of duration of BSO treatment was statistically significant ($p < 0.001$ by ANOVA). *Significantly different from 0 h control, $p < 0.001$ by LSD test.

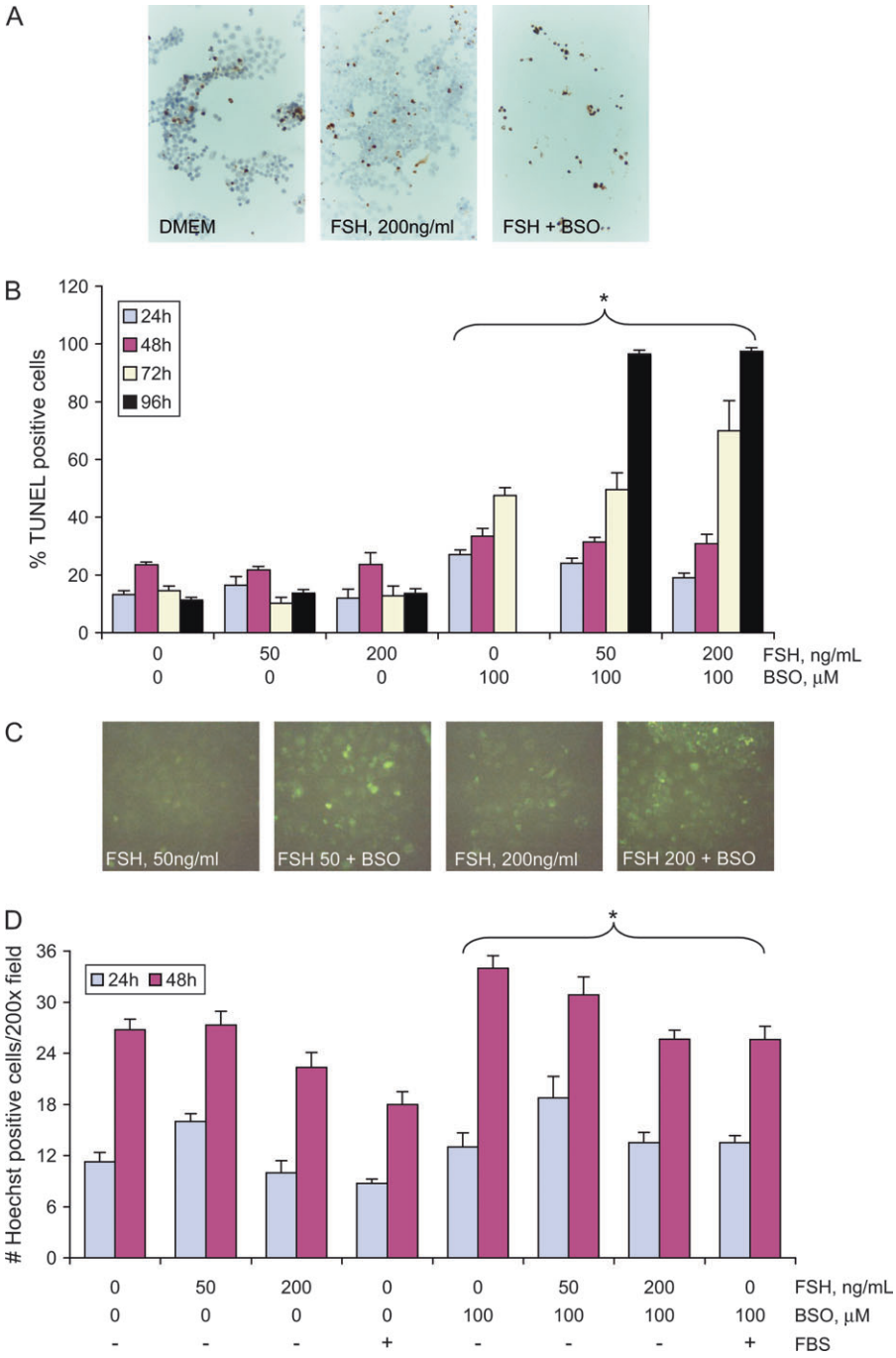

FIG. 3. Depletion of GSH with BSO induces apoptosis, as assessed by TUNEL and Hoechst staining, within 24 h. COV434 cells were cultured in (1) DMEM F12 medium alone, (2) 50 ng/ml FSH, (3) 200 ng/ml FSH, (4) 100μM BSO, (5) 50 ng/ml FSH plus 100μM BSO, or (6) 200 ng/ml FSH plus 100μM BSO. For Hoechst staining there were two additional treatment groups, (1) DMEM with 9% FBS and (2) DMEM 9% FBS with 100μM BSO. At the end of the indicated treatment periods, cells were fixed and processed for TUNEL or Hoechst 33342 staining as described in ''Materials and Methods.'' (A) Representative images of COV434 cells cultured for 96 h with the indicated treatments. TUNEL-positive cells are stained brown; cells are counterstained with hematoxylin. Note the few remaining cells in the FSH + BSO panel, nearly all of which are TUNEL positive. Original magnification ×66. (B) The graph shows the percentage + SEM of TUNEL-positive cells counted per ×400 field. The effect of BSO was statistically significant at every time point by two-way ANOVA ($p < 0.004$). The effect of FSH was not statistically significant at any time point. Because the Levene's test showed nonhomogeneity of variances for the 72 and 96 h ANOVAs, nonparametric analyses were also performed. The effect of treatment was statistically significant at all time points by Kruskal–Wallis test ($p < 0.008$). $N = 4$–12 per group. (C) Representative images of Hoechst 33342 staining in COV434 cells cultured for 24 h with the indicated treatments. Original magnification ×66. (D) The graph shows the mean + SEM of Hoechst-positive cells counted per ×200 field. The effects of FSH ($p < 0.002$) and BSO (*$p < 0.004$) were statistically significant at both time points by three-way ANOVA. The effect of FBS was significant at 48 h only ($p = 0.001$). $N = 4$–8 per group.

intense nuclear staining and fragmentation by Hoechst staining (Zhivotovsky and Orrenius, 2001). For these experiments, two additional treatment groups of cells cultured with medium supplemented with 9% FBS with or without BSO were included to assess whether the addition of serum would be more protective against apoptosis induced by GSH depletion than FSH treatment. There was a statistically significant increase in the number of apoptotic cells by Hoechst staining already after 24 h of culture with BSO, with or without concomitant FSH or serum treatment, and the number of Hoechst-positive cells increased further after 48 h of BSO treatment ($p < 0.004$, effect of BSO by three-way ANOVA at both time points; Figs. 3C and 3D). There was also a statistically significant effect of FSH treatment, with fewer Hoechst-positive cells in the 200 ng/ml FSH-treated groups compared to cells cultured with DMEM F12 alone ($p = 0.001$, effect of FSH dose; Fig. 3D). Culture in medium with serum also appeared to be slightly protective against apoptosis, but this was statistically significant only at 48 h ($p = 0.001$, effect of serum).

Surprisingly, in light of the TUNEL and Hoechst results, no oligonucleosomal DNA fragmentation was observed by agarose gel electrophoresis at 24, 48, 72, or 96 h of culture in any treatment group (not shown).

Effect of FSH and BSO Treatment on COV434 Cell Viability

Treatment with BSO for 24, 48, 72, and 96 h significantly decreased cell viability, as assessed by WST-1 assay ($p < 0.003$, effect of treatment at 24, 48, 72, and 96 h by Kruskal–Wallis test; Fig. 4). Intergroup comparisons revealed significantly lower cell viability in nearly every BSO-treated group at every time point, compared to the respective non-BSO–treated control. At 24 h, FSH appeared to increase the number of viable cells ($p = 0.033$ and $p = 0.061$, 50 ng/ml FSH and 200 ng/ml FSH, respectively, vs. DMEM control by Mann–Whitney test). However, there was no effect of treatment with 50 or 200 ng/ml FSH or modulation of the effect of BSO by FSH on cell viability at any of the later time points.

4HC Treatment Induces Apoptosis in COV434 Granulosa Cells

Preliminary experiments with 10 to 500μM cyclophosphamide for 48–96 h did not increase apoptosis in COV434 cells as judged by only a minimal, nonstatistically significant, decrease in cell viability at the highest dose, suggesting that these cells do not efficiently metabolize cyclophosphamide to its active metabolites (data not shown). We therefore used 4HC, a preactivated form of cyclophosphamide (Flowers *et al.*, 2000; Gamcsik *et al.*, 1999) for the subsequent experiments.

Treatment for 12 or 24 h with 4HC induced apoptosis in COV434 cells in a dose- and time-dependent manner, as measured both by TUNEL ($p < 0.001$, effect of 4HC dose by Kruskal–Wallis test at both time points; Fig. 5A) and by Hoechst staining ($p < 0.01$, effect of dose at both time points; Fig. 5B). Treatment of COV434 cells with 4HC caused a dose-dependent appearance of activated (cleaved) caspase 3 protein at 12 and 24 h (Fig. 5C). 4HC treatment also led to statistically significant decreases in cell viability, as measured by WST cleavage ($p < 0.001$, effect of dose by Kruskal–Wallis test at both time points; Fig. 5D). *Post hoc* comparisons revealed that the lowest dose of 4HC (1μM) induced a statistically significant decrease in cell viability already at 12 h (Fig. 5D).

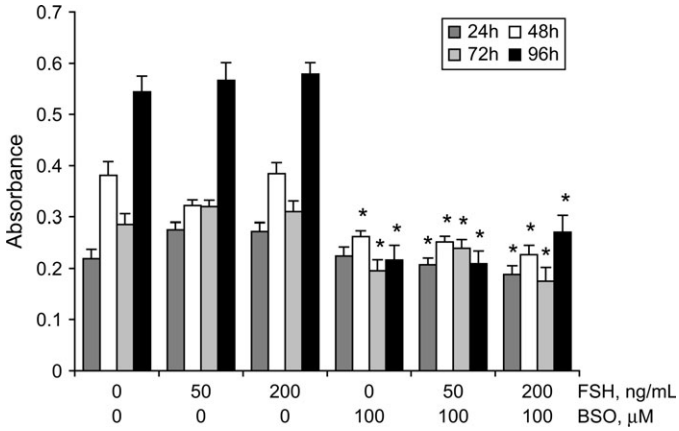

FIG. 4. Depletion of GSH with BSO significantly decreases COV434 cell viability within 24 h. COV434 cells were treated as for Figure 3. At the end of the indicated treatment periods, cells were processed for WST-1 cell viability assay as described in "Materials and Methods." The graph shows the mean + SEM of the WST absorbance readings. The effect of treatment was statistically significant at every time point by Kruskal–Wallis test ($p < 0.003$). *Significantly different from respective non-BSO–treated control by Mann–Whitney test, $p < 0.05$. $N = 12$–15 per group.

Oligonucleosomal DNA fragmentation was not evident on DNA gel electrophoresis of DNA extracted from COV434 cells treated with 0–50μM 4HC for 24 h (data not shown).

4HC Treatment Increases ROS Formation in COV434 Cells

ROS generation, measured as the slope of the increase in DCF fluorescence, was continuously monitored during 2 h treatment with 0, 1, 10, or 50μM 4HC or 500μM hydrogen peroxide as a positive control. There was a statistically significant effect of treatment on ROS generation during the 2-h incubation ($p < 0.001$, by 1-way ANOVA; Fig. 6A). ROS levels in the 50μM 4HC and H_2O_2 groups were significantly greater than in the 0μM 4HC controls. ROS were also measured using DCF-DA after 6 h incubation with 0, 1, 10, or 50μM 4HC. DCF fluorescence increased significantly in groups treated with 1, 10, and 50μM 4HC for 6 h compared to 0μM controls ($p < 0.001$, effect of 4HC by Kruskal–Wallis test, Fig. 6B).

4HC Treatment Causes Oxidative DNA Damage in COV434 Cells

To test whether the rise in ROS caused by treatment with 4HC causes oxidative DNA damage, we used 8-OHdG immunostaining. The number of 8-OHdG–positive cells increased in a

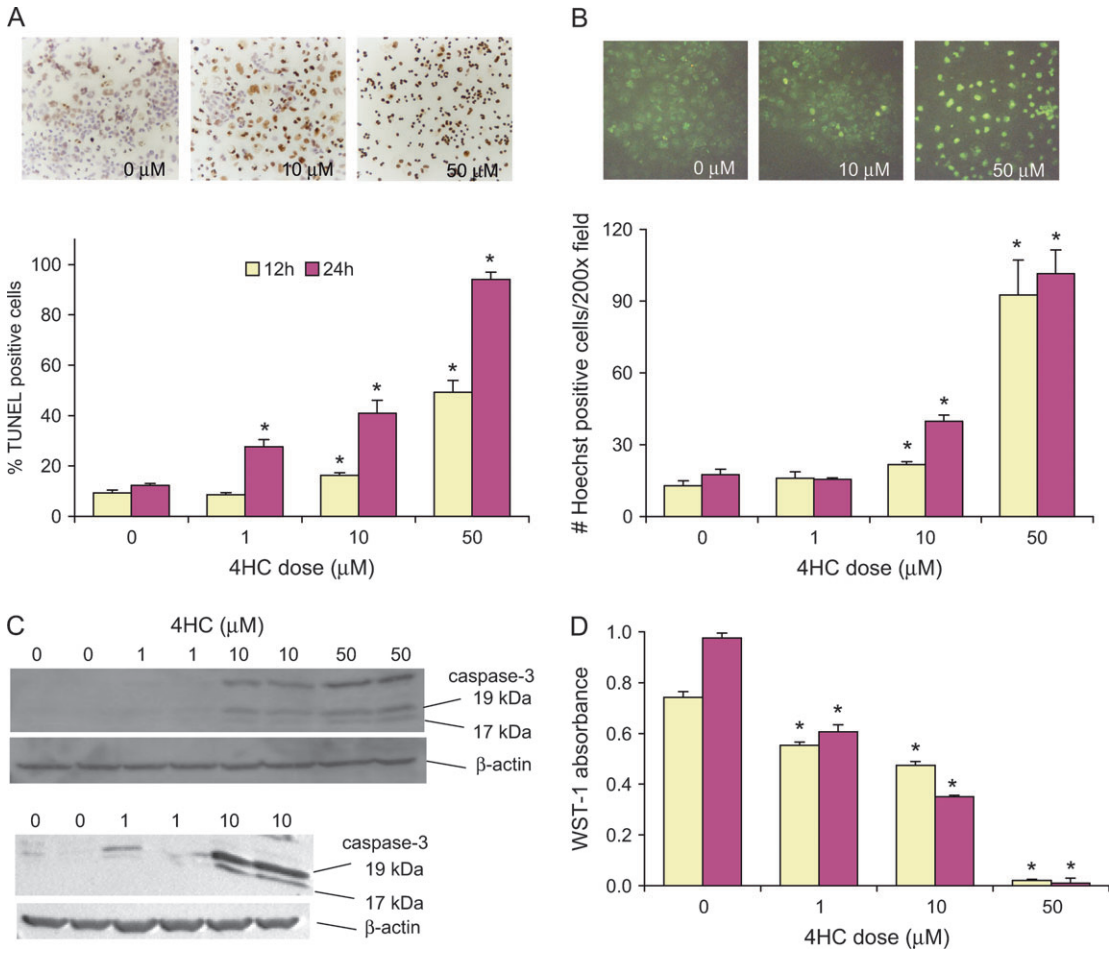

FIG. 5. 4HC treatment induces apoptosis within 12 h in COV434 cells. COV434 cells were treated with 0, 1, 10, or 50μM 4HC. At the end of the indicated treatment periods cells were fixed and processed for TUNEL (A) or Hoechst 33342 (B) staining, were collected for protein extraction and Western analysis (C), or were processed for WST-1 cell viability assay (D), as described in "Materials and Methods." (A) Representative bright field images of cells treated with the indicated doses of 4HC for 24 h are shown at top. TUNEL-positive cells are stained brown; cells are counterstained with hematoxylin. Original magnification ×66. The graph shows the mean + SEM percentage of TUNEL-positive cells per ×400 field. The effect of treatment was statistically significant at both time points ($p < 0.001$ by Kruskal–Wallis test). $N = 8$ per group. (B) Representative fluorescence images of cells treated with the indicated doses of 4HC for 24 h are shown at top. Hoechst-positive cells have bright green condensed or fragmented nuclei. Original magnification ×66. The graphs show the mean + SEM number of Hoechst 33342–positive cells per ×200 field. The effect of treatment was statistically significant at both time points ($p < 0.010$ by Kruskal–Wallis test). $N = 4$ per group. (C) Images of representative Western blots of protein extracts from COV434 cell samples collected after 12 (bottom) or 24 h (top) of treatment with 4HC. Treatment with 4HC activated caspase 3, as indicated by the appearance of the cleaved 17 and 19 kDa forms of caspase 3. The 12-h blot was exposed to film for a longer duration than the 24-h blot in order to visualize the cleaved caspase 3 bands. Blots were reprobed with β-actin antibody to verify equal protein loading. (D) The graph shows the mean + SEM WST-1 absorbance values for $N = 12$ per group. The effect of treatment was statistically significant at both time points ($p < 0.001$ by Kruskal–Wallis test). *Significantly different from respective non-BSO–treated control by Mann–Whitney test, $p < 0.05$.

dose-dependent manner after 12 h of 4HC treatment ($p < 0.001$, effect of dose by Kruskal–Wallis test, Fig. 7).

4HC Treatment Depletes Total Intracellular GSH in COV434 Cells

Treatment of cultured hepatic sinusoidal endothelial cells with 4HC or hepatocytes with cyclophosphamide caused a rapid decline in intracellular GSH concentrations that preceded the onset of cell death (DeLeve, 1996). Prevention of this decline in GSH concentrations also protected against cell killing by cyclophosphamide (DeLeve, 1996). To determine whether the induction of COV434 cell apoptosis by 4HC also involves the depletion of GSH, we measured intracellular GSH concentrations at different times after 4HC treatment.

Treatment of COV434 cells with 50μM 4HC caused a rapid decline in total intracellular GSH concentrations by 2 h compared to control 0μM cells (Fig. 8A; $p = 0.002$, $p < 0.001$, effect of 4HC by Kruskal–Wallis test at 2 and 4h, respectively). Treatment with 10μM 4HC caused a small, statistically significant decrease in GSH levels at 4 h only (Fig. 8A). The decline in GSH concentrations at 2 h in the 50μM

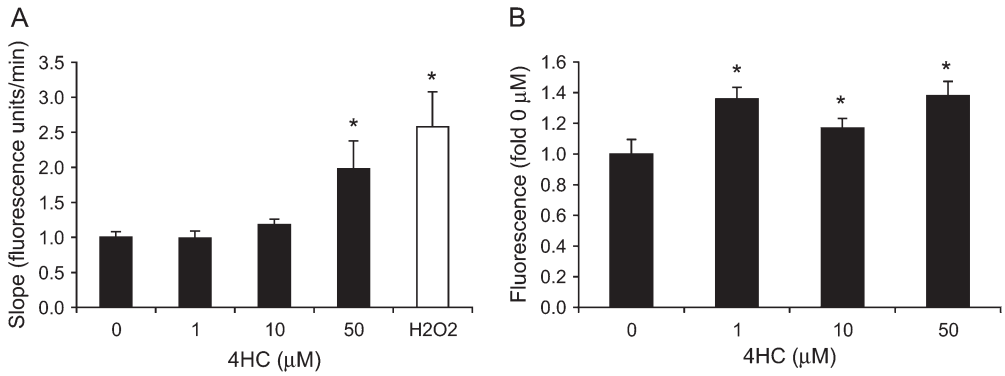

FIG. 6. 4HC treatment generates ROS. (A) COV434 cells were loaded with 100μM DCF-DA for 30 min, then incubated with the indicated doses of 4HC in HBSS or with 500μM hydrogen peroxide (H_2O_2) as a positive control while the fluorescence intensity was measured every 5 min for 2 h. The graph shows the mean + SEM of the slopes of the fluorescence increases expressed as fold the mean of the controls. The effect of treatment was statistically significant ($p < 0.001$, by Kruskal–Wallis test; *significantly different from 0μM 4HC control by Mann–Whitney test; $N = 24$ per group, except H_2O_2, $N = 12$). (B) COV434 cells were treated with the indicated doses of 4HC for 6 h. After 30 min incubation with 100μM DCF-DA, fluorescence intensity was measured as described in ''Materials and Methods.'' The data from two replicate experiments were combined for analysis. The graph shows the mean + SEM of the fluorescence intensity expressed as fold the mean of the 0μM 4HC controls. The effect of 4HC was statistically significant ($p < 0.001$, by Kruskal–Wallis test; *significantly different from 0μM 4HC control by Mann–Whitney test, $p < 0.001$; $N = 24$ per group).

group preceded an increase in cell death at 4 h, which was not statistically significant due to high variability in the percentage of dead cells in the 50μM group (Fig. 8E). GSSG concentrations also declined by 2 h of treatment with 50μM 4HC, but the effect of treatment was not statistically significant (Fig. 8B). The ratio of rGSH/GSSG decreased significantly after 2 and 4 h of treatment with 50μM 4HC ($p = 0.002$, effect of 4HC at 2 and 4 h by Kruskal–Wallis test; Fig. 8D). The GSH reduction potential (E_h) became significantly more positive (oxidized) after 2 and 4 h of 50μM 4HC treatment ($p = 0.001$, effect of 4HC by Mann–Whitney test at 2 and 4 h; Fig. 8E).

To assess whether longer duration of treatment with lower doses of 4HC would cause a further decline in GSH concentrations, cells were treated with 1 or 10μM 4HC for 8 or 12 h. There was no effect of 4HC treatment on total intracellular GSH concentrations at either time point (Fig. 9A), despite a small, but statistically significant increase in cell death ($p < 0.001$, effect of 4HC dose; Fig. 9B).

Supplementation of GSH or Treatment with Other Antioxidants Suppresses 4HC-Induced Apoptosis

To test whether the depletion of GSH or the generation of ROS mediates the induction of apoptosis by 4HC, we cotreated cells with 50μM 4HC and a cell-permeable form of GSH, GEE, or with the thiol antioxidant DTT or with AA for 24 h. Treatment with AA, DTT, or GEE alone significantly increased apoptosis, measured by TUNEL, in the absence of 4HC treatment (Fig. 10). This effect was greatest for AA and minimal for GEE. As expected, 50μM 4HC induced apoptosis in nearly 100% of the cells by 24 h. This effect was significantly suppressed by all three antioxidants, but most effectively by GEE and DTT (Fig. 10; $p < 0.01$ 4HC + antioxidant groups vs. 4HC by Mann–Whitney test).

Depletion of GSH with BSO Sensitizes COV434 Cells to 4HC-Induced Apoptosis

To test whether GSH depletion enhances the toxicity of 4HC to COV434 cells, the cells were treated with 0, 1, or 10μM 4HC

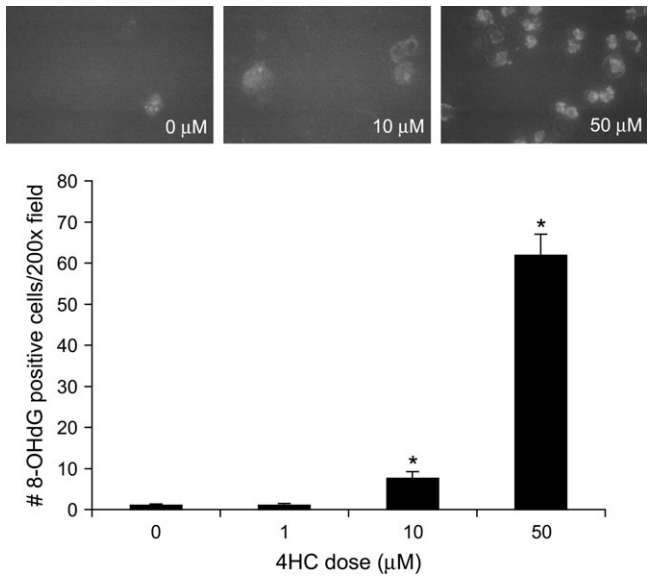

FIG. 7. 4HC treatment causes oxidative DNA damage in COV434 cells. COV434 cells were treated as for Figure 5. After 12 h of treatment, cells were fixed and processed for 8-OHdG immunofluorescence as described in ''Materials and Methods.'' Fluorescence microscope images show representative 8-OHdG staining in cells treated with the indicated doses of 4HC. Only rare fluorescent cells are observed in the control 0μM image; many fluorescent cells are observed in the 50μM image. Original magnification ×132. The graph shows means + SEM of the number of 8-OHdG–positive cells per ×200 field. The effect of 4HC dose was statistically significant ($p < 0.001$ by Kruskal–Wallis test). *Significantly different from 0μM 4HC control by Mann–Whitney test, $p < 0.01$.

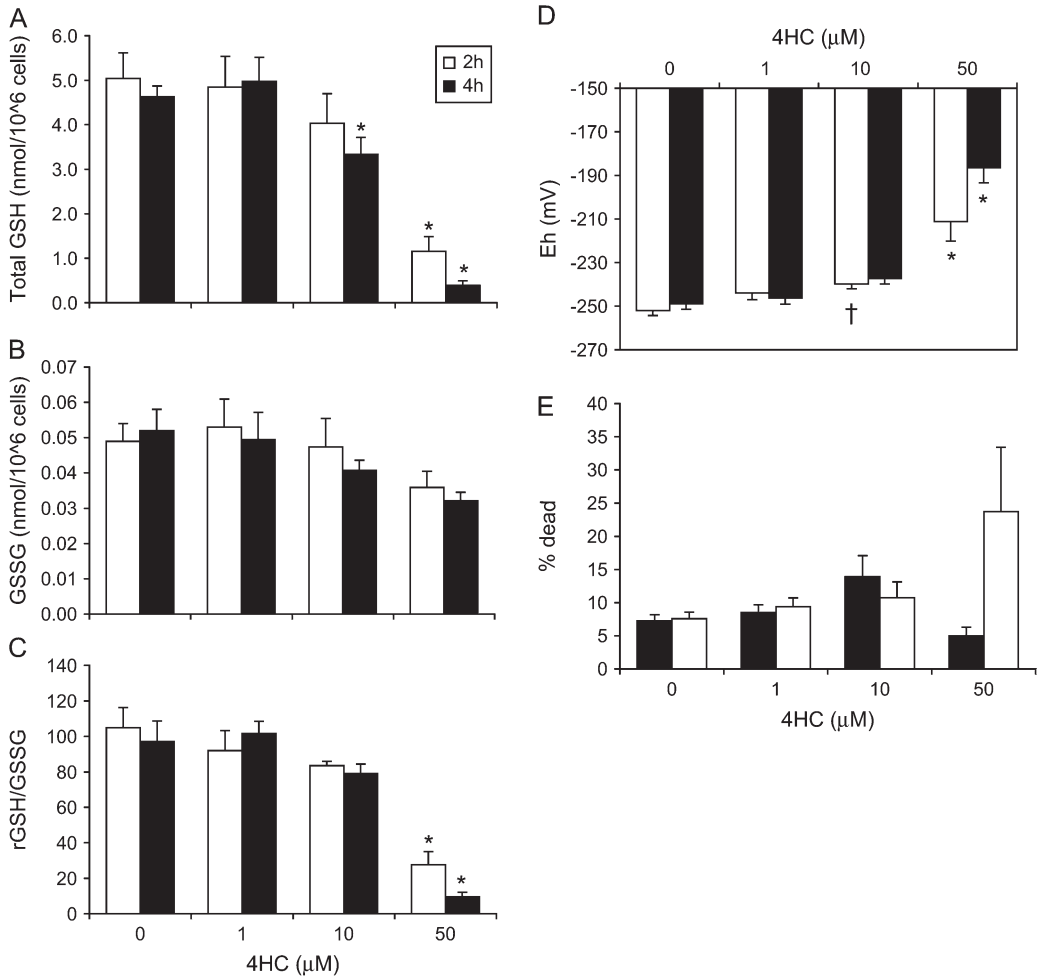

FIG. 8. 4HC treatment dose-dependently depletes total intracellular GSH concentrations, decreases the ratio of rGSH to GSSG, and oxidizes the GSSG/2rGSH reduction potential. COV434 cells were treated with the indicated doses of 4HC for 2 or 4 h. Total intracellular GSH and GSSG were measured and the concentration of rGSH and the GSSG/2rGSH reduction potential (E_h) were calculated, as described in ''Materials and Methods.'' The data from four independent experiments were pooled for analysis ($N = 5$–10 per group). (A) Mean + SEM total intracellular GSH. The effect of 4HC treatment was statistically significant by Kruskal–Wallis test at both time points ($p = 0.002$, $p < 0.001$ at 2 and 4 h, respectively; *significantly different from respective 0μM 4HC control by Mann–Whitney test, $p < 0.01$). (B) Mean + SEM GSSG. The effect of treatment was not statistically significant. (C) Mean + SEM rGSH/GSSG. The effect of treatment was statistically significant at both time points by Kruskal–Wallis test ($p = 0.002$, $p = 0.002$ at 2 and 4 h, respectively; *significantly different from 0μM 4HC control by Mann–Whitney test, $p < 0.001$). (D) Mean + SEM GSSG/2rGSH reduction potential, E_h. The effect of treatment was statistically significant at both time points by Kruskal–Wallis test ($p = 0.001$, $p = 0.001$ at 2 and 4 h, respectively; significantly different from 0μM 4HC control by Mann–Whitney test, *$p < 0.001$, †$p < 0.05$). (E) Mean + SEM percentage of dead cells, determined by trypan blue exclusion. The effect of treatment was not statistically significant at either time point by Kruskal–Wallis test.

alone or in combination with 100μM BSO. Treatment with 4HC alone caused a dose-dependent and statistically significant increase in apoptosis that became more pronounced with increasing duration of treatment, as judged by both TUNEL ($p < 0.001$, effect of 4HC dose by three-way ANOVA; Fig. 11A) and Hoechst staining ($p < 0.001$, effect of 4HC dose; Fig. 11B). Cotreatment with BSO increased apoptosis as assessed by TUNEL ($p < 0.001$, effect of BSO, Fig. 11A) and Hoechst staining ($p < 0.001$, effect of BSO by three-way ANOVA) in 4HC treated cells as well as in control cells not treated with 4HC. For each 4HC dose and time point, there were more apoptotic cells with BSO than without. The effect of 4HC on cell viability (Fig. 11C) was similarly enhanced by cotreatment with BSO ($p \leq 0.001$, effect of 4HC dose, effect of BSO, effect of time by three-way ANOVA).

To assess whether the effect of GSH depletion would be more pronounced if GSH levels were already suppressed when 4HC was added to the cultures, cells were treated for 8 h with 100μM BSO, followed by treatment with 1 or 10μM 4HC for 12 or 24 h (Fig. 12). The effects of treatment with 4HC and with BSO on the number of apoptotic cells as judged by TUNEL and Hoechst staining were highly statistically significant ($p < 0.001$, effect of 4HC, effect of BSO by three-way ANOVA). The number of Hoechst-positive cells at both time

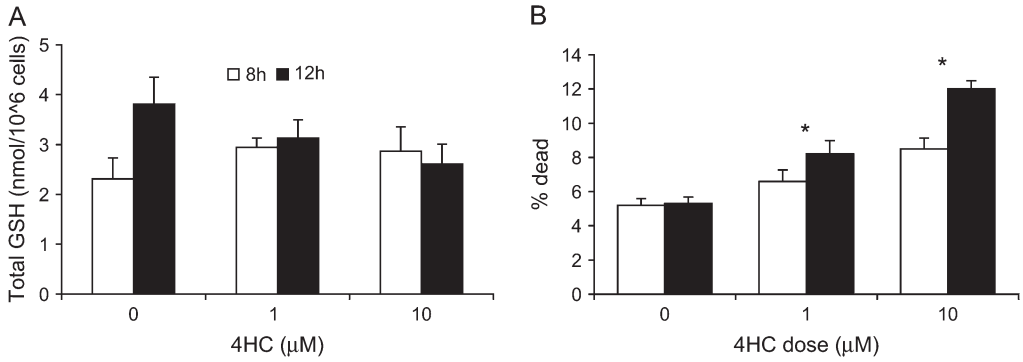

FIG. 9. Total intracellular GSH concentrations are not suppressed further after longer treatment with 1 or 10μM 4HC. COV434 cells were treated with 0, 1, or 10μM 4HC for 8 or 12 h and were processed for total GSH assay. Numbers of live and dead cells were counted using Trypan Blue exclusion. (A) Mean + SEM total intracellular GSH concentrations at the indicated times after onset of treatment. The effects of 4HC dose and treatment duration were not statistically significant by two-way ANOVA. (B) Mean + SEM percentage of dead cells at the indicated times after onset of treatment. The effects of 4HC dose and of treatment duration were statistically significant by two-way ANOVA on the arcsine square root transformed data ($p < 0.001$, $p = 0.002$, respectively). $N = 9$ per group. *statistically significantly different from 0μM 4HC by Fisher's LSD test at $p < 0.05$.

points was greater in the groups treated with both 4HC and BSO than the sum of the number of positive cells in the groups treated with either compound alone ($p = 0.012$, 4HC × BSO interaction). Similarly, pretreatment with BSO significantly enhanced the percentage of cells that were TUNEL positive at both doses of 4HC ($p < 0.001$, 4HC × BSO interaction).

DISCUSSION

Cyclophosphamide treatment causes temporary amenorrhea or permanent ovarian failure in women (Howell and Shalet, 1998; Kumar *et al.*, 1972). In rodents cyclophosphamide destroys primordial and primary ovarian follicles as well as preantral and antral follicles (Davis and Heindel, 1998; Plowchalk and Mattison, 1991, 1992; Shiromizu *et al.*, 1984). In primordial and small primary follicles, cyclophosphamide appears to target the oocytes for apoptotic destruction, whereas in larger follicles, cyclophosphamide induces granulosa cell apoptosis followed by death of the oocyte (Desmeules and Devine, 2006; Lopez and Luderer, 2004). In the current study we have used a human granulosa cell tumor line and a preactivated form of cyclophosphamide, 4HC, to investigate the mechanism by which cyclophosphamide induces apoptosis in granulosa cells and to examine the role of GSH in granulosa cell apoptosis. We demonstrated that 4HC dose-dependently induced apoptosis in COV434 human granulosa cells and that the induction of apoptosis by 4HC was associated with caspase 3 activation. 4HC-induced apoptosis was preceded by increased ROS levels, decreased ratio of reduced to oxidized glutathione (GSSG), and by oxidation of the GSSG/2rGSH reduction potential. Together with the observation that 4HC caused oxidative DNA damage, these results show that 4HC treatment induces oxidative stress in COV434 cells. Cotreatment with antioxidants protected against 4HC-induced apoptosis. We also showed that 4HC-induced apoptosis was preceded by depression of intracellular GSH concentrations, that GSH depletion using BSO induced apoptosis, and that combined treatment with BSO and 4HC more than additively induced apoptosis. Together these findings provide strong evidence that GSH depletion mediates 4HC-induced apoptosis in COV434 cells via the induction of oxidative stress.

The observations in the present study that 4HC treatment (Fig. 5) and GSH depletion with BSO (Fig. 3) induced apoptosis in a human granulosa cell line are consistent with our previous observations in rat granulosa cells. Treatment of adult female rats with cyclophosphamide caused granulosa cell apoptosis in secondary and antral follicles within 24 h (Lopez and Luderer, 2004). This apoptosis after *in vivo* treatment with cyclophosphamide was associated with activation of caspase 9 and caspase 3 in granulosa cells (unpublished data). Similarly, in

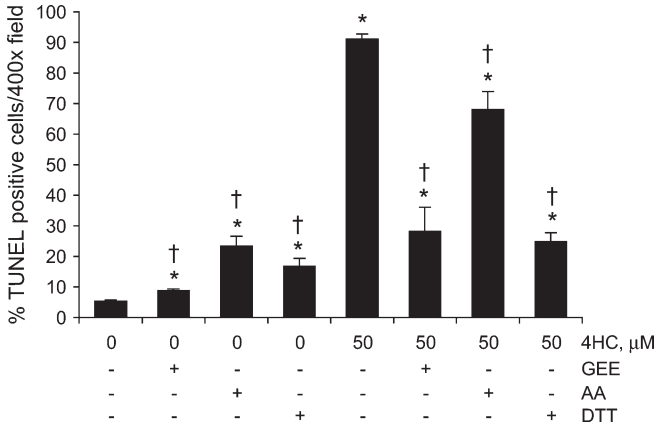

FIG. 10. Cotreatment with antioxidants prevents 4HC-induced apoptosis. COV434 cells were cultured with or without 50μM 4HC in the absence or presence of 5mM GEE, 0.5mM DTT, or 1mM AA. After 24 h, cells were fixed and processed for TUNEL. The graph shows the mean + SEM percentage of TUNEL-positive cells per ×400 field. The effect of treatment was statistically significant by Kruskal–Wallis test ($p = 0.001$). *Significantly different from untreated control, †significantly different from 4HC, $p < 0.01$ by Mann–Whitney test. $N = 8$ per group.

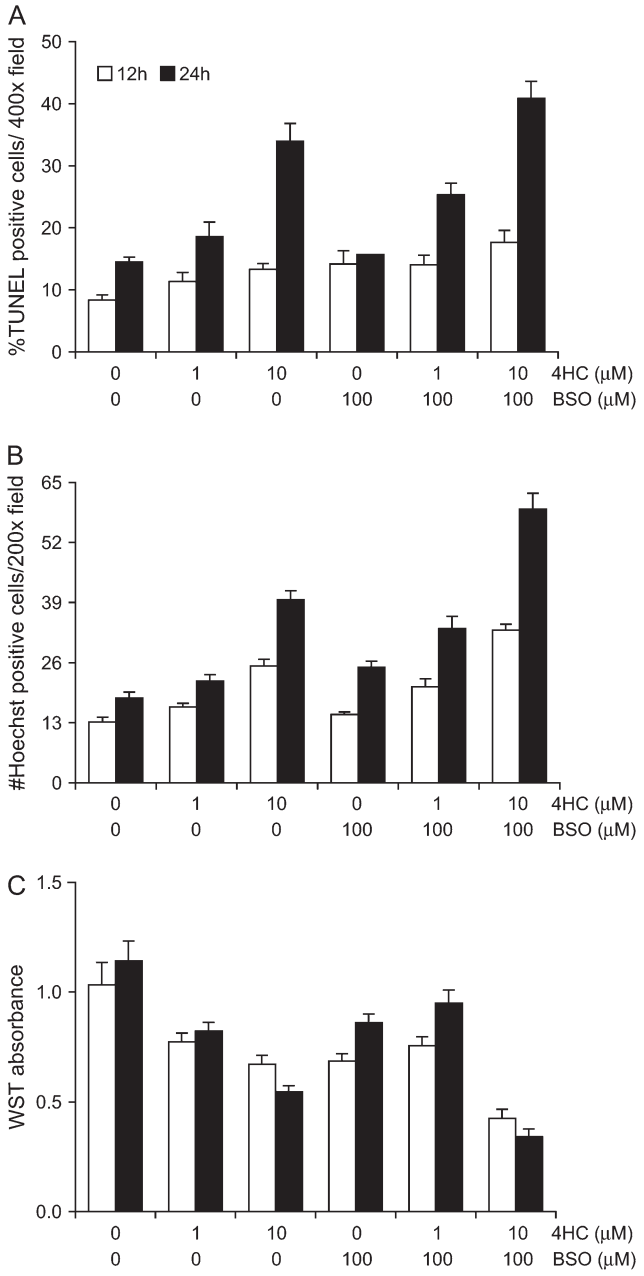

FIG. 11. GSH depletion with BSO enhances the induction of apoptosis by 4HC in COV434 cells: 4HC and BSO treatment initiated at the same time. COV434 cells were cultured with DMEM F12, 9% FBS alone or with the indicated doses of 4HC and BSO. After the indicated durations of treatment, cells were fixed and processed for identification of apoptosis by TUNEL (A) or Hoechst 33342 staining (B) or were processed for WST-1 cell viability assay (C). (A) Mean + SEM of the percentage of TUNEL-positive cells per treatment group and time point. The effects of 4HC dose ($p < 0.001$), BSO ($p < 0.001$), and duration of treatment ($p < 0.001$) were statistically significant by three-way ANOVA on the arcsine square root transformed percentages. The interaction term 4HC dose × duration of treatment was also statistically significant ($p < 0.001$). $N = 7$–8 per group. (B) Mean + SEM number of Hoechst 33342–positive cells per treatment and time point. The effects of 4HC ($p < 0.001$), BSO ($p < 0.001$), and duration of treatment ($p < 0.001$) were statistically significant by three-way ANOVA on the natural log transformed counts. The interaction term 4HC dose × BSO was also statistically significant ($p = 0.048$). $N = 8$ per group. (C) Mean + SEM WST-1 absorbance. The effects of 4HC ($p < 0.001$), BSO ($p = 0.001$), and duration of treatment ($p = 0.001$) were statistically significant by three-way ANOVA. The interaction terms 4HC dose × BSO and 4HC dose × time were also statistically significant ($p < 0.001$). Because the variances were not homogeneous, Kruskal–Wallis tests were also performed for each time point with Mann–Whitney tests for *post hoc* comparisons. These tests also showed that the effect of treatment was statistically significant at both time points ($p < 0.001$, $p < 0.001$ at 12 and 24 h, respectively). $N = 24$ per group.

the present experiments treatment of human COV434 granulosa cells with 4HC was associated with caspase 3 activation. *In vivo* treatment with BSO led to a significant increase in antral follicle atresia (Lopez and Luderer, 2004), and treatment of cultured preovulatory rat follicles with BSO increased granulosa cell apoptosis (Tsai-Turton and Luderer, 2006). GSH depletion alone has also been reported to induce apoptosis in some cultured cell lines (Anderson *et al.*, 1999; Celli *et al.*, 1998; Higuchi and Matsukawa, 1999; Merad-Boudia *et al.*, 1998).

Unlike COV434 cells and the other cell lines mentioned above, GSH depletion alone did not induce apoptosis in pancreatic cancer cells (Schnelldorfer *et al.*, 2000), HL-60 or PW cells overexpressing Bcl-2 (Wright *et al.*, 1998), HeLa cells (Jungas *et al.*, 2002), or nonsmall cell lung cancer cells (Honda *et al.*, 2004), but GSH depletion sensitized these cells to other proapoptotic stimuli. In the current study, we observed that GSH depletion with BSO slightly, but statistically significantly, enhanced the induction of apoptosis by 4HC when BSO and 4HC treatment were initiated at the same time (Fig. 11). Because it takes several hours after BSO treatment for intracellular GSH levels to fall (Fig. 2B), we tested whether pretreatment with BSO for 8 h prior to initiating 4HC treatment would augment this potentiating effect of BSO. Pretreatment with BSO, followed by the addition of 4HC indeed led to greater potentiation of 4HC-induced apoptosis (Fig. 12) than was observed when the treatments were initiated simultaneously.

Oligonucleosomal DNA fragmentation, yielding the characteristic DNA ladder pattern on DNA gel electrophoresis, is often considered a hallmark of apoptosis. However, despite TUNEL and Hoechst 33342 staining and caspase 3 activation, we did not observe DNA laddering in COV434 cells treated with 4HC or BSO alone. The only other study of which we are aware in which apoptosis was studied in COV434 cells assessed apoptosis by morphological changes and by flow cytometry analysis after staurosporine treatment (Zhang *et al.*, 2005). Oligonucleosomal DNA fragmentation was not evaluated in that study. Others have reported that oligonucleosomal DNA fragmentation is not required for apoptotic cell death, whereas high molecular weight DNA fragmentation, resulting from the excision of nuclear loop domains, appears to be a necessary step for the initiation of apoptosis (Oberhammer *et al.*, 1993; Solovyan *et al.*, 1998). In a human T-lymphoblastic leukemia cell line, treatment with the antineoplastic drug

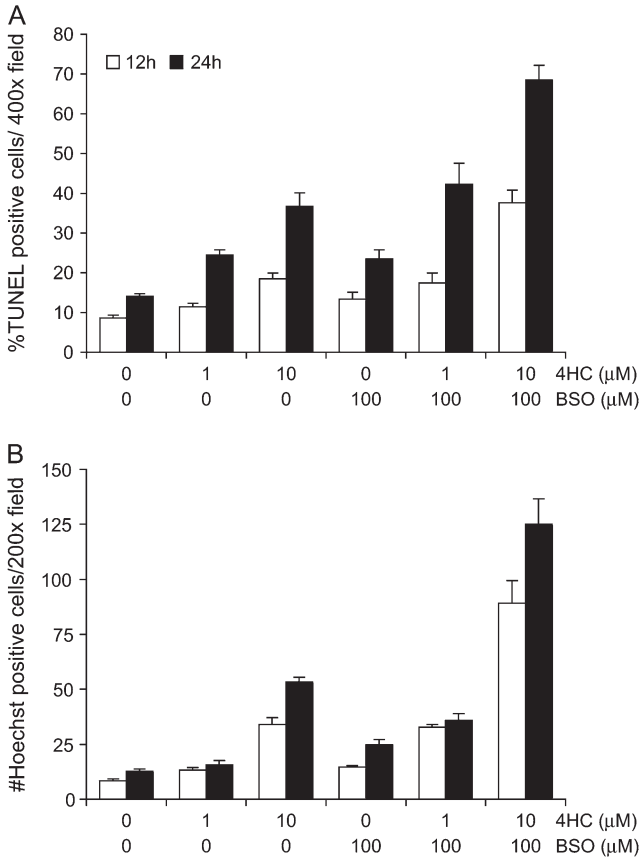

FIG. 12. GSH depletion with BSO enhances the induction of apoptosis by 4HC in COV434 cells: BSO treatment initiated 8 h before 4HC treatment. COV434 cells were cultured with DMEM F12, 9% FBS alone, or with 100μM BSO. After 8 h of pretreatment with BSO, 4HC or an equal volume of medium was added to bring the final concentration to 0, 1, or 10μM 4HC, and culture was continued for 12 or 24 additional hours. Cells were then fixed and processed for identification of apoptosis by TUNEL (A) or Hoechst 33342 staining (B). (A) Mean + SEM of the percentage of TUNEL-positive cells per treatment group and time point. The effects of 4HC dose, BSO, duration of treatment, and 4HC × BSO interaction were statistically significant by three-way ANOVA on the arcsine square root transformed percentages (all $p < 0.001$). $N = 4$–8 per group. (B) Mean + SEM number of Hoechst 33342–positive cells per treatment and time point. The effects of 4HC ($p < 0.001$), BSO ($p < 0.001$), duration of treatment ($p < 0.001$), and 4HC × BSO interaction ($p = 0.012$) were statistically significant by three-way ANOVA on the natural log transformed counts. $N = 4$–8 per group.

1-β-D-arabinofuranosylcytosine (ara-C) caused high molecular weight DNA fragmentation, which was followed by lower molecular weight DNA fragmentation that did not exhibit the characteristic oligonucleosomal fragmentation pattern (Badran *et al.*, 2003). In these experiments, lower molecular weight DNA fragmentation was confirmed by TUNEL and by the detection of a subpopulation of cells with less than 2*N* DNA complement by flow cytometry (Badran *et al.*, 2003). Moreover, significant increases in caspase 3 enzymatic activity were also detected in these cells (Badran *et al.*, 2003). We conclude that cell death in the present experiments was indeed apoptotic, but that COV434 cells may not undergo oligonucleosomal DNA fragmentation during apoptosis. Unlike the similarities noted above between granulosa cell apoptosis in rodent models and COV434 cell apoptosis in the present study, the lack of oligonucleosomal DNA fragmentation in COV434 cells constitutes a difference between these two models. Rat granulosa cells exhibit oligonucleosomal DNA fragmentation during apoptosis *in vivo* and *in vitro* (Tilly *et al.*, 1992; Trbovich *et al.*, 1998; Zeleznik *et al.*, 1989). The lack of a prominent anti-apoptotic effect of FSH treatment is another difference between the COV434 cells and cultured primary rat follicles (Chun *et al.*, 1994, 1996; Tsai-Turton and Luderer, 2006) and primary human luteinized granulosa cells (Matsubara *et al.*, 2000). These differences suggest that primary human granulosa cells may respond differently to GSH depletion or 4HC treatment than COV434 cells, and we plan to explore this in future experiments.

Treatment of COV434 cells with 4HC significantly depressed intracellular GSH concentrations. This is consistent with previous reports that cyclophosphamide or 4HC treatment depleted GSH concentrations in other cell types. Treatment of hepatic sinusoidal epithelial cells with 4HC was reported to cause 95% depletion of GSH and a significant increase in cell death within 6 h (DeLeve, 1996). Treatment of cultured hepatocytes with cyclophosphamide also resulted in GSH depletion and cell death, and prevention of the decline in GSH protected against cell killing (DeLeve, 1996). *In vivo* treatment of mice with cyclophosphamide has also been reported to result in rapid depletion of bone marrow, liver, and blood GSH concentrations that was maximal at 24 h (Adams *et al.*, 1985). A mechanistic role for active GSH extrusion from cells has been proposed by Coppola and Ghibelli (2000) in the mitochondrial apoptotic pathway. These workers showed that GSH extrusion from cells preceded cytochrome *c* release, that inhibition of GSH extrusion with methionine or cystathionine inhibited apoptosis induced by puromycin, and that GSH depletion with BSO also caused cytochrome c release (Coppola and Ghibelli, 2000; Ghibelli *et al.*, 1999). Taken together, our observations that depleting GSH with BSO-induced apoptosis, that 4HC caused depletion of GSH prior to the onset of apoptosis, that GSH supplementation with GEE prevented 4HC-induced apoptosis, and that GSH depletion with BSO enhanced the apoptotic effect of 4HC suggest that GSH depletion mediates the induction of apoptosis by 4HC in COV434 cells.

In the present study we observed that 4HC treatment of COV434 cells caused declines in the ratio of reduced GSH to GSSG and oxidation of the GSSG/2rGSH reduction potential by 2 h (Fig. 8), increased ROS by 2 h (Fig. 6), and caused oxidative DNA damage by 12 h of treatment (Fig. 7). Furthermore, cotreatment with the antioxidants GEE, DTT, or AA prevented 4HC-induced apoptosis (Fig. 10). These findings provide strong evidence that 4HC initiates apoptosis in granulosa cells by inducing oxidative stress. The increase in ROS appears to be due to the depletion of GSH, since levels of GSSG did not increase, but rather declined, with 4HC treatment. Others have observed increased levels of lipid peroxidation in

bronchoalveolar lavage fluid (Venkatesan and Chandrakasan, 1995) and in the liver (Berrigan *et al.*, 1987) after *in vivo* treatment with cyclophosphamide. Murata *et al.* (2004) reported that treatment of HL-60 cells for 2 h with a dose of 4HC that also induced apoptosis led to a significant increase in 8-OHdG formation. In contrast, these workers reported no apoptosis or significantly increased 8-OHdG formation when the cells were treated with cyclophosphamide. There are several possible explanations for these apparently discordant observations. One explanation is that 4HC decomposition liberates hydrogen peroxide as well as 4-hydroxycyclophosphamide, which spontaneously converts to phosphoramide mustard and other metabolites of cyclophosphamide, whereas treatment with cyclophosphamide itself does not generate hydrogen peroxide. Murata *et al.* (2004) provided evidence that hydrogen peroxide was generated upon treatment of HL-60 cells with 4HC, but did not assess hydrogen peroxide generation after cyclophosphamide treatment. Another, not mutually exclusive explanation is that HL-60 cells do not possess the cytochrome P450 enzymes required to metabolize cyclophosphamide to 4-hydroxycyclophosphamide. The latter explanation seems to be plausible, as CYP3A4, -2B6, -2C8, and -2C9 were undetectable by reverse transcription-polymerase chain reaction in untreated HL-60 cells (Kawai *et al.*, 2003; Nagai *et al.*, 2002). On the other hand, the presence of mRNA for CYP2A6 in HL-60 cells (Nagai *et al.*, 2002) suggests that they may possess at least one of the cytochrome P450 enzymes that is active in metabolizing cyclophosphamide (Chang *et al.*, 1993). The cytochrome P450 expression profiles of COV434 cells have not been investigated, but the lack of significant cell death upon treatment with cyclophosphamide in our preliminary experiments suggests that COV434 cells lack the ability to metabolize cyclophosphamide.

In summary, we have shown that that treatment of COV434 human granulosa cells with 4HC caused oxidative stress, as indicated by oxidative DNA damage, DCF fluorescence, and decreased ratio of reduced GSH to GSSG, and induced apoptosis subsequent to depressing total intracellular GSH concentrations. We further showed that GSH depletion by inhibition of its synthesis using BSO induced apoptosis, that BSO enhanced the apoptotic effect of 4HC treatment, and that antioxidants prevented the apoptotic effect of 4HC on COV434 granulosa cells. These findings are consistent with roles for oxidative stress and GSH depletion in mediating the induction of apoptosis in COV434 granulosa cells by cyclophosphamide. Future studies will investigate whether these findings are also applicable to the induction of apoptosis by cyclophosphamide in primary human granulosa cells.

ACKNOWLEDGMENTS

We are grateful to Dr Susan Ludeman for the gift of the 4HC and to Dr Peter Schrier for the gift of the COV434 cells. This work was funded by National Institutes of Health grant ES10963 to U.L. and by the Center for Occupational and Environmental Health, University of California Irvine. B.T.L. received a UC Irvine Undergraduate Research Opportunities Program grant to carry out some experiments described herein.

REFERENCES

Adams, D. J., Carmichael, J., and Wolf, C. R. (1985). Altered mouse bone marrow glutathione and glutathione transferase levels in response to cytotoxins. *Cancer Res.* **45,** 1669–1673.

Anderson, C. P., Tsai, J. M., Meek, W. E., Liu, R.-M., Tang, Y., Forman, H. J., and Reynolds, C. P. (1999). Depletion of glutathione by buthionine sulfoximine is cytotoxic for human neuroblastoma cell lines via apoptosis. *Exp. Cell Res.* **246,** 183–192.

Badran, A., Iwasaki, H., Inoue, H., and Ueda, T. (2003). Atypical nuclear apoptosis downstream to caspase-3 activation in Ara-C treated CCRF-CEM cells. *Int. J. Oncol.* **22,** 517–522.

van den Berg-Bakker, C. A. M., Hegemeijer, A., Franken-Meijer, A., Franken-Postma, E. M., Smit, V. T. H. B. M., Kuppen, P. J. K., Ravenswaay-Claasen, H. H., Cornelisse, C. J., and Schrier, P. I. (1993). Establishment and characterization of 7 ovarian carcinoma cell lines and one granulosa tumor cell line: Growth features and cytogenetics. *Int. J. Cancer* **53,** 613–620.

Berrigan, M. J., Struck, R. F., and Gurtoo, H. L. (1987). Lipid peroxidation induced by cyclophosphamide. *Cancer Biochem. Biophys.* **9,** 265–270.

Celli, A., Que, F. G., Gores, G. J., and LaRusso, N. F. (1998). Glutathione depletion is associated with decreased Bcl-2 expression and increased apoptosis in cholangiocytes. *Am. J. Physiol.* **275,** G749–G757.

Chang, T. K., Weber, G. F., Crespi, C. L., and Waxman, D. J. (1993). Differential activation of cyclophosphamide and ifosphamide by cytochromes P-450 2B and 3A in human liver microsomes. *Cancer Res.* **53,** 5629–5637.

Chun, S.-Y., Billig, H., Tilly, J. L., Furuta, I., Tsafriri, A., and Hsueh, A. J. W. (1994). Gonadotropin suppression of apoptosis in cultured preovulatory follicles: Mediatory role of endogenous insulin-like growth factor I. *Endocrinology* **135,** 1845–1853.

Chun, S. Y., Eisenhauer, K. M., Minami, S., Billig, H., Perlas, E., and Hsueh, A. J. (1996). Hormonal regulation of apoptosis in early antral follicles: Follicle-stimulating hormone as a major survival factor. *Endocrinology* **137,** 1447–1456.

Coppola, S., and Ghibelli, L. (2000). GSH extrusion and the mitochondrial pathway of apoptotic signaling. *Biochem. Soc. Trans.* **28**(Part 2), 56–61.

Dalton, T. P., Chen, Y., Schneider, S. N., Nebert, D. W., and Shertzer, H. G. (2004). Genetically altered mice to evaluate glutathione homeostasis in health and disease. *Free Radic. Biol. Med.* **37,** 1511–1526.

Davis, B. J., and Heindel, J. J. (1998). Ovarian toxicants: Multiple mechanisms of action. In *Reproductive and Developmental Toxicology* (K. S. Korach, Ed.), pp. 373–395. Marcel Dekker, Inc., New York.

DeLeve, L. D. (1996). Cellular target of cyclophosphamide toxicity in the murine liver: Role of glutathione and site of metabolic activation. *Hepatology* **24,** 830–837.

Desmeules, P., and Devine, P. J. (2006). Characterizing the ovotoxicity of cyclophosphamide metabolites on cultured mouse ovaries. *Toxicol. Sci.* **90,** 500–509.

Dhar, A., Dockery, P., O, W. S., Turner, K., Lenton, E. A., and Cooke, I. D. (1996). The human ovarian granulosa cell: A stereological approach. *J. Anat.* **188,** 671–676.

Dirven, H. A. A. M., van Ommen, B., and van Bladeren, P. J. (1994). Involvement of human glutathione S-transferase isoenzymes in the conjugation of cyclophosphamide metabolites with glutathione. *Cancer Res.* **54,** 6215–6220.

Flowers, J., Ludeman, S. M., Gamcsik, M. P., Colvin, O. M., Shao, K.-L., Boal, J. H., Springer, J. B., and Adams, D. J. (2000). Evidence for a role of chloroethylaziridine in the cytotoxicity of cyclophosphamide. *Cancer Chemother. Pharmacol.* **45,** 335–344.

Gamcsik, M. P., Dolan, M. E., Andersson, B. S., and Murray, D. (1999). Mechanisms of resistance to the toxicity of cyclophosphamide. *Curr. Pharm. Des.* **5,** 587–605.

Ghibelli, L., Coppola, S., Fanelli, C., Rotilio, G., Civitareale, P., Scovassi, A. I., and Ciriolo, M. R. (1999). Glutathione depletion causes cytochrome c release even in the absence of cell commitment to apoptosis. *FASEB J.* **13,** 2031–2036.

Griffith, O. W. (1980). Determination of glutathione and glutathione disulfide using glutathione reductase and 2-vinylpyridine. *Anal. Biochem.* **106,** 207–212.

Higuchi, Y., and Matsukawa, S. (1999). Glutathione depletion induces giant DNA and high-molecular-weight DNA fragmentation associated with apoptosis through lipid peroxidation and protein kinase C activation in C6 glioma cells. *Arch. Biochem. Biophys.* **363,** 33–42.

Honda, T., Coppola, S., Ghibelli, L., Cho, S. H., Kagawa, S., Spurgers, K. B., Roth, J. A., Meyn, R. E., Fang, B., and McDonnell, T. J. (2004). GSH depletion enhances adenoviral Bax-induced apoptosis in lung cancer cells. *Cancer Gene Ther.* **11,** 249–255.

Howell, S., and Shalet, S. (1998). Gonadal damage from chemotherapy and radiotherapy. *Endocrinol. Metab. Clin. North Am.* **27,** 927–943.

Jungas, T., Motta, I., Duffieux, F., Fanen, P., Stoven, V., and Ojcius, D. M. (2002). Glutathione levels and BAX activation during apoptosis due to oxidative stress in cells expressing wild-type and mutant cystic fibrosis transmembrane conductance regulator. *J. Biol. Chem.* **277,** 27912–27913.

Kawai, M., Chen, J., Cheung, C. Y. S., and Chang, T. K. H. (2003). Transcript profiling of cytochrome P450 HL-60 human leukemic cells: Upregulation of CYP1B1 by all-trans-retinoic Acid. *Mol. Cell. Biochem.* **248,** 57–65.

Kirlin, W. G., J., C., Thompson, S. A., Diaz, D., Kavanagh, T. J., and Jones, D. P. (1999). Glutathione redox potential in response to differentiation and enzyme inducers. *Free Radic. Biol. Med.* **27,** 1208–1218.

Kumar, R., Biggart, J. D., McEvoy, J., and McGeown, M. G. (1972). Cyclophosphamide and reproductive function. *Lancet* **June 3,** 1212–1214.

Lindner, G., Botchkarev, V. A., Botchkareva, N. V., Ling, G., van der Veen, C., and Paus, R. (1997). Analysis of apoptosis during hair follicle regression (catagen). *Am. J. Pathol.* **151,** 1601–1617.

Little, S. A., and Mirkes, P. E. (2002). Teratogen-induced activation of caspase-9 and the mitochondrial apoptotic pathway in early post-implantation mouse embryos. *Toxicol. Appl. Pharmacol.* **181,** 142–151.

Lopez, S. G., and Luderer, U. (2004). Effects of cyclophosphamide and buthionine sulfoximine on ovarian glutathione and apoptosis. *Free Radic. Biol. Med.* **36,** 1366–1377.

Luderer, U., Diaz, D., Faustman, E. M., and Kavanagh, T. J. (2003). Localization of glutamate cysteine ligase subunit mRNA within the rat ovary and relationship to follicular atresia. *Mol. Reprod. Dev.* **65,** 254–261.

Luderer, U., Kavanagh, T. J., White, C. C., and Faustman, E. M. (2001). Gonadotropin regulation of glutathione synthesis in the rat ovary. *Reprod. Toxicol.* **15,** 495–504.

Matsubara, H., Ikuta, K., Ozaki, Y., Suzuki, Y., Suzuki, N., Sata, T., and Suzumori, K. (2000). Gonadotropins and cytokines affect luteal function through control of apoptosis in human luteinized granulosa cells. *J. Clin. Endocrinol. Metab.* **85,** 1620–1626.

Merad-Boudia, M., Nicole, A., Santiard-Baron, D., Saillé, C., and Ceballos-Picot, I. (1998). Mitochondrial Impairment as an early event in the process of apoptosis induced by glutathione depletion in neuronal cells: Relevance to Parkinson's disease. *Biochem. Pharmacol.* **56,** 645–655.

Mirkes, P. E., and Little, S. A. (2000). Cytochrome c release from mitochondria of early postimplantation murine embryos exposed to 4-hydroperoxycyclophosphamide, heat shock, and staurosporine. *Toxicol. Appl. Pharmacol.* **162,** 197–206.

Murata, M., Suzuki, T., Midorikawa, K., Oikawa, S., and Kawanishi, S. (2004). Oxidative DNA damage induced by a hydroperoxide derivative of cyclophosphamide. *Free Radic. Biol. Med.* **37**, 793–802.

Nagai, F., Hiyoshi, Y., Sugimachi, K., and Tamura, H.-O. (2002). Cytochrome P450 (CYP) Expression in human myeloblastic and lymphoid cell lines. *Biol. Pharm. Bull.* **25,** 383–385.

Oberhammer, F., Wilson, J. W., Dive, C., Morris, I. D., Hickman, J. A., Wakeling, A. E., Walker, P. R., and Sikorska, M. (1993). Apoptotic death in epithelial cells: Cleavage of DNA to 300 and/or 50 kb fragments prior to or in absence of internucleosomal DNA fragmentation. *EMBO J.* **12,** 3679–3684.

Pasternack, B. S., and Shore, R. E. (1982). Analysis of dichotomous response data from toxicological experiments involving stable laboratory mouse populations. *Biometrics* **38,** 1057–1067.

Plowchalk, D. R., and Mattison, D. R. (1991). Phosphoramide mustard is responsible for the ovarian toxicity of cyclophosphamide. *Toxicol. Appl. Pharmacol.* **107,** 472–481.

Plowchalk, D. R., and Mattison, D. R. (1992). Reproductive toxicity of cyclophosphamide in the C57BL/6N mouse: 1. Effects on ovarian structure and function. *Reprod. Toxicol.* **6,** 411–421.

Puri, R. N., and Meister, A. (1983). Transport of glutathione as γ-glutamylcysteinylglycyl ester into liver and kidney. *Proc. Natl. Acad. Sci. U. S. A.* **80,** 5258–5260.

Ren, S., Kalhorn, T. F., McDonald, G. B., Anasetti, C., Appelbaum, F. R., and Slattery, J. T. (1998). Pharmacokinetics of cyclophosphamide and its metabolites in bone marrow transplantation patients. *Clin. Pharmacol. Ther.* **64,** 289–301.

Royall, J. A., and Ischiropoulos, H. (1993). Evaluation of 2',7'-dichlorofluorescin and dihydrorhodamine 123 as fluorescent probes for intracellular H_2O_2 in cultured endothelial cells. *Arch. Biochem. Biophys.* **302,** 348–355.

Schafer, F. Q., and Buettner, G. R. (2001). Redox environment of the cell as viewed through the redox state of the glutathione disulfide/glutathione couple. *Free Radic. Biol. Med.* **30,** 1191–1212.

Schnelldorfer, T., Gansauge, S., Gansauge, F., Schlosser, S., Beger, H. G., and Nussler, A. K. (2000). Glutathione depletion causes cell growth inhibition and enhanced apoptosis in pancreatic cancer cells. *Cancer* **89,** 1440–1447.

Shen, D., Dalton, T. P., Nebert, D. W., and Shertzer, H. G. (2005). Glutathione redox state regulates mitochondrial reactive oxygen production. *J. Biol. Chem.* **280,** 25305–25312.

Shiromizu, K., Thorgeirsson, S. S., and Mattison, D. R. (1984). Effect of cyclophosphamide on oocyte and follicle number in Sprague-Dawley rats, C57BL/6N and DBA/2N mice. *Pediatr. Pharmacol.* **4,** 213–221.

Solovyan, V., Bezvenyuk, Z., Huotari, V., Tapiola, T., Suuronen, T., and Salminen, A. (1998). Distinct mode of apoptosis induced by genotoxic agent etoposide and serum withdrawal in neuroblastoma cells. *Brain Res. Mol. Brain Res.* **62,** 43–55.

Tilly, J. L., Billig, H., Kowalski, K. I., and Hsueh, A. J. W. (1992). Epidermal growth factor and basic fibroblast growth factor suppress the spontaneous onset of apoptosis in cultured rat ovarian granulosa cells and follicles by a tyrosine kinase-dependent mechanism. *Mol. Endocrinol.* **6,** 1942–1950.

Trbovich, A. M., Hughes, F. M., Jr, Perez, G. I., Kugu, K., Tilly, K. I., Cidlowski, J. A., and Tilly, J. L. (1998). High and low molecular weight DNA cleavage in ovarian granulosa cells: Characterization and protease modulation in intact cells and in cell-free nuclear autodigestion assays. *Cell Death Differ.* **5,** 38–49.

Tsai-Turton, M., and Luderer, U. (2005). Gonadotropin regulation of glutamate cysteine ligase catalytic and modifier subunit expression in the rat ovary is subunit and follicle stage-specific. *Am. J. Physiol.* **289,** E391–E402.

Tsai-Turton, M., and Luderer, U. (2006). Opposing effects of glutathione depletion and FSH on reactive oxygen species and apoptosis in cultured preovulatory rat follicles. *Endocrinology* **147,** 1224–1236.

Venkatesan, N., and Chandrakasan, G. (1995). Modulation of cyclophosphamide-induced early lung injury by curcumin, an anti-inflammatory antioxidant. *Mol. Cell. Biochem.* **142,** 79–87.

Wang, H., and Joseph, J. A. (1999). Quantifying cellular oxidative stress by dichlorofluorescein assay using microplate reader. *Free Radic. Biol. Med.* **27,** 612–616.

Wright, S. C., Wang, H., Wei, Q. S., Kinder, D. H., and Larrick, J. W. (1998). Bcl-2-mediated resistance to apoptosis is associated with glutathione-induced inhibition of AP24 activation of nuclear DNA fragmentation. *Cancer Res.* **58,** 5570–5576.

Zeleznik, A. J., Ihrig, L. L., and Bassett, S. G. (1989). Developmental expression of Ca++/Mg++-dependent endonuclease activity in rat granulosa and luteal cells. *Endocrinology* **125,** 2218–2220.

Zhang, H., Vollmer, M., De Geyter, M., Dürrenberger, M., and De Geyter, C. (2005). Apoptosis and differentiation induced by staurosporine in granulosa tumor cells is coupled with activation of JNK and suppression of p38 MAPK. *Int. J. Oncol.* **26,** 1575–1580.

Zhang, H., Vollmer, M., De Geyter, M., Litzistorf, Y., Ladewig, A., Dürrenberger, M., Guggenheim, R., Miny, P., Holzgreve, W., and De Geyter, C. (2000). Characterization of an immortalized human granulosa cell line (COV434). *Mol. Hum. Reprod.* **6,** 146–153.

Zhivotovsky, B., and Orrenius, S. (2001). Assessment of apoptosis and necrosis by DNA fragmentation and morphological criteria. In *Current Protocols in Cell Biology* (J. S. Bonifacino, M. Dasso, J. B. Harford, J. Lippincott-Schwartz, and K. M. Yamada, Eds.), pp. 18.3.1–18.3.23. John Wiley and Sons, Inc, Hoboken, NJ.